



ELSEVIER

Biophysical Chemistry 93 (2001) 215–230

Biophysical  
Chemistry

www.elsevier.com/locate/bpc

# Heat does not come in different colours: entropy–enthalpy compensation, free energy windows, quantum confinement, pressure perturbation calorimetry, solvation and the multiple causes of heat capacity effects in biomolecular interactions

Alan Cooper<sup>a,\*1</sup>, Christopher M. Johnson<sup>b</sup>, Jeremy H. Lakey<sup>c</sup>,  
Marcelo Nöllmann<sup>a</sup>

<sup>a</sup>*Department of Chemistry, Joseph Black Building, University of Glasgow, Glasgow G12 8QQ, Scotland, UK*

<sup>b</sup>*MRC Centre for Protein Engineering, Hills Road, Cambridge, CB2 2QH, UK*

<sup>c</sup>*Department of Biochemistry and Genetics, The Medical School, University of Newcastle-upon-Tyne, Newcastle-upon-Tyne, NE2 4HH, UK*

Received 23 March 2001; accepted 3 May 2001

## Abstract

Modern techniques in microcalorimetry allow us to measure directly the heat changes and associated thermodynamics for biomolecular processes in aqueous solution at reasonable concentrations. All these processes involve changes in solvation/hydration, and it is natural to assume that the heats for these processes should reflect, in some way, such changes in solvation. However, the interpretation of data is still somewhat ambiguous, since different non-covalent interactions may have similar thermodynamic signatures, and analysis is frustrated by large entropy–enthalpy compensation effects. Changes in heat capacity ( $\Delta C_p$ ) have been related to changes in hydrophobic hydration and non-polar accessible surface areas, but more recent empirical and theoretical work has shown how this need not always be the case. Entropy–enthalpy compensation is a natural consequence of finite  $\Delta C_p$  values and, more generally, can arise as a result of quantum confinement effects, multiple weak interactions, and limited free energy windows, giving rise to thermodynamic homeostasis that may be of evolutionary and functional advantage.

\* Corresponding author. Tel.: +44-141-330-5278; fax: +44-141-330-2910.

E-mail address: alanc@chem.gla.ac.uk (A. Cooper).

<sup>1</sup> www: <http://www.chem.gla.ac.uk/staff/alanc/>

The new technique of pressure perturbation calorimetry (PPC) has enormous potential here as a means of probing solvation-related volumetric changes in biomolecules at modest pressures, as illustrated with preliminary data for a simple protein-inhibitor complex. © 2001 Elsevier Science B.V. All rights reserved.

*Keywords:* Microcalorimetry; Heat changes; Thermodynamics

## 1. Introduction

Modern techniques in microcalorimetry allow us to directly measure the heat changes and associated thermodynamics for biomolecular processes in aqueous solution at reasonable concentrations. Using isothermal titration microcalorimetry (ITC) we can directly probe the thermodynamics of protein–ligand, protein–protein, and protein–DNA interactions for example. Using differential scanning calorimetry (DSC) we can observe the heat energy uptake in processes such as protein unfolding and helix-coil transitions. All these processes involve changes in solvation/hydration, and it is natural to assume that the heats for these processes should reflect, in some way, such changes in solvation. However, the interpretation of data is still somewhat ambiguous [1,2]. The problem arises because there is no characteristic thermal signature of the different kinds of non-covalent interactions and associated solvation effects responsible for biomolecular stability and interactions. A typical system comprises a multitude of weakly interacting groups, involving interactions variously described in terms of hydrogen bonding, van der Waals/dispersion forces, hydrophobic, and other polar and non-polar thermodynamic interactions in which the dynamics of solvent molecules are intimately involved. Different contributions may be endothermic or exothermic, depending on circumstances, and there are no straightforward ways of dissecting out the individual contributions. Moreover, the individual enthalpic ( $\Delta H$ ) and entropic ( $\Delta S$ ) contributions can vary enormously, but often in a compensatory fashion, to give relatively smaller variations in the free energy ( $\Delta G$ ) that ultimately determines the thermodynamic stability of any process. Such entropy–enthalpy compensation is a source of considerable frustration in the thermodynamic understanding of macromolecular interactions. Here

we will review briefly the calorimetric background and discuss a number of fundamental reasons why such entropy–enthalpy compensation and related thermodynamic properties are inevitable in systems such as these. We shall also present preliminary data using the new technique of pressure perturbation calorimetry (PPC) that might help resolve some of the ambiguities.

## 2. Microcalorimetry: the thermodynamics of protein stability and interaction

Typical experimental data from differential scanning (DSC) and isothermal titration (ITC) calorimetry are given in Figs. 1 and 2, illustrating the kind of measurements now routinely possible for biomolecules in solution. DSC is useful for investigating thermal transitions in solution [3,4] and has been widely applied to study the thermodynamics of protein folding [5]. In favourable circumstances, unfolding transitions with protein concentrations as low as 0.2 mg/ml may be measured, and for simple cooperative reversible processes the complete thermodynamics of the transition may be obtained (Fig. 3a). ITC directly measures the heat changes upon addition of small volumes (5–10  $\mu\text{l}$ ) of one solution to another in the calorimetric cell (1–2 ml), and is typically used to study protein–ligand binding or protein–protein interactions [6–8]. In dilution mode it may also be used to determine monomer–dimer or oligomer–dissociation equilibrium parameters [9]. Since (almost) all interaction processes involve heat change in one form or other, ITC may be applied simply as a convenient, non-invasive, non-destructive analytical method for determining binding stoichiometry ( $n$ ) and affinity ( $K$ ). But in addition, for those interested in the fundamental thermodynamics of such

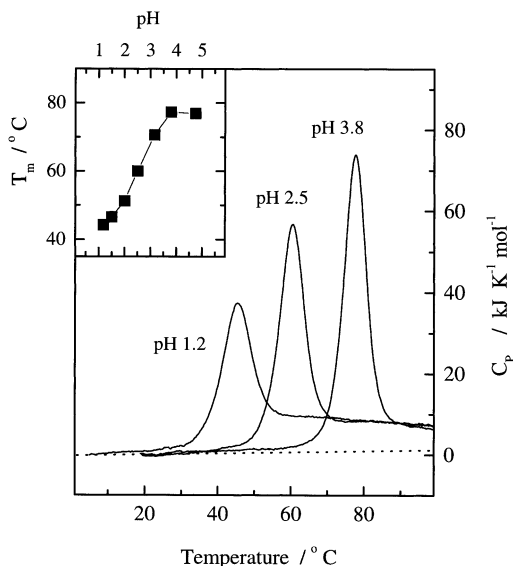


Fig. 1. Typical DSC data for the unfolding of a small globular protein (lysozyme) in solution at various pH values. The insert shows the variation in mid-point unfolding temperature ( $T_m$ ) as a function of pH. The increase in area under each endotherm with higher  $T_m$ , and the higher heat capacity base-lines after the unfolding transitions, are both indications of the significant positive  $\Delta C_p$  commonly associated with such processes.

processes, it yields enthalpy data ( $\Delta H$ ) which, together with free energy ( $\Delta G^{\circ} = -RT \ln K$ ), allows calculation of entropy ( $\Delta S^{\circ}$ ) and, given temperature dependent data, the heat capacity change ( $\Delta C_p$ ) for the process as well. Typical thermodynamic data for a protein–protein interaction are illustrated in Fig. 3b (see, e.g. [10–12]). All these examples illustrate the strong temperature dependence of both  $\Delta H$  and  $\Delta S$ , a consequence of the large  $\Delta C_p$  effects that are a common feature of many biomolecular and other interactions in solution. Despite such large variations in entropy and enthalpy, the free energy change upon which equilibrium stability ultimately depends is relatively much less affected. This almost ubiquitous ‘entropy–enthalpy compensation’ (see below) leads to considerable difficulty in rationalising the large number of quite detailed studies involving careful mutagenesis and structural analysis in terms of the underlying thermodynamic forces [2].

### 3. The origins of ubiquitous entropy–enthalpy compensation

Entropy–enthalpy compensation effects have been noted in many earlier studies, with the particular significance in biomolecular systems highlighted by the classic work of Lumry and Rajender [13], and the phenomenon has given rise to much subsequent discussion (summarised recently in [14]). This substantial body of work shows how large changes in enthalpy ( $\Delta H$ ) and entropy ( $\Delta S$ ) with variation of experimental conditions (particularly temperature) frequently ap-

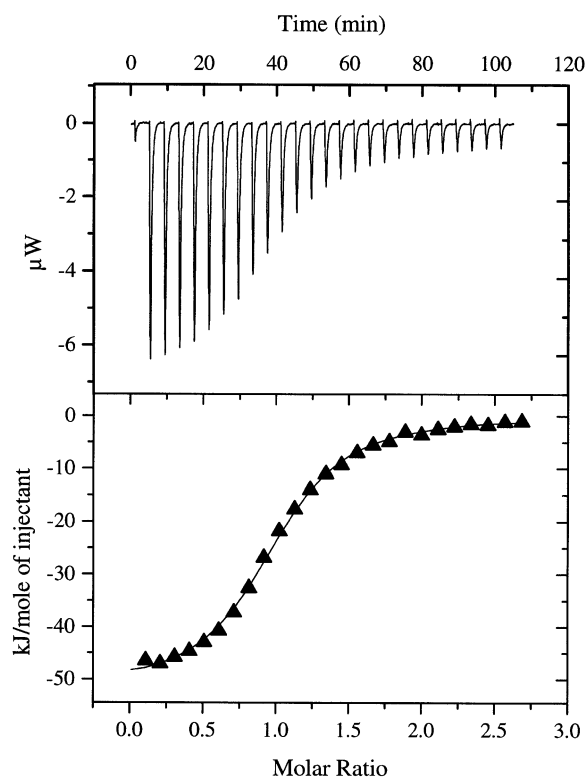


Fig. 2. Typical ITC data for binding of a trisaccharide inhibitor (tri-*N*-acetyl-glucosamine; tri-NAG) to hen egg white lysozyme, in 0.1 M acetate buffer, pH 5. Each exothermic heat pulse (upper panel) corresponds to injection of 10  $\mu\text{l}$  of tri-NAG (0.45 mM) into the protein solution (36  $\mu\text{M}$ ). Integrated heat data (lower panel) constitute a differential binding curve that may be fit to a standard single-site binding model to give, in this instance, the stoichiometry of binding,  $N = 0.99$ , binding affinity,  $K_{\text{ass}} = 3.9 \times 10^5 \text{ M}^{-1}$  ( $K_{\text{diss}} = 2.6 \mu\text{M}$ ), and enthalpy of binding,  $\Delta H = -51.7 \text{ kJ mol}^{-1}$ .

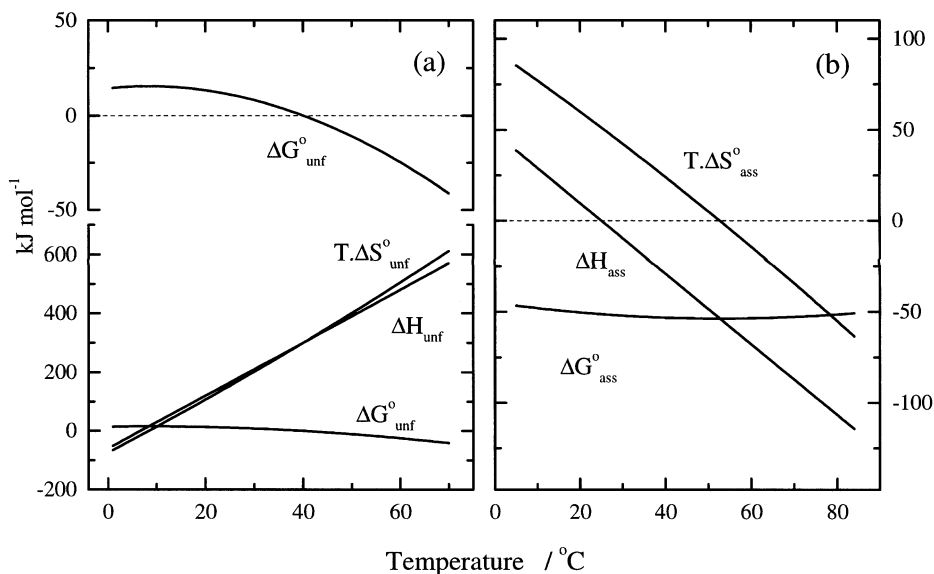


Fig. 3. Typical thermodynamic parameters as a function of temperature for biomolecular processes determined by microcalorimetry. (a) Free energy ( $\Delta G_{\text{unf}}^{\circ}$ ), enthalpy ( $\Delta H_{\text{unf}}^{\circ}$ ) and entropy ( $T\Delta S_{\text{unf}}^{\circ}$ ) of unfolding in solution of a typical globular protein, with heat capacity increment upon infolding,  $\Delta C_p = 9 \text{ kJ K}^{-1} \text{ mol}^{-1}$ . The free energy data are also shown expanded in the upper panel, for clarity. (b) Free energy ( $\Delta G_{\text{ass}}^{\circ}$ ), enthalpy ( $\Delta H_{\text{ass}}^{\circ}$ ) and entropy ( $T\Delta S_{\text{ass}}^{\circ}$ ) of association interaction between protein subunits in solution. In this case the strong temperature dependence of the enthalpy (heat) of binding corresponds to a  $\Delta C_p$  value of  $-1.9 \text{ kJ K}^{-1} \text{ mol}^{-1}$ , typical of many such interactions [10–12], and shows how the enthalpy may even change sign, being endothermic at low temperatures but exothermic at higher temperatures.

pear to be correlated in such a manner as to compensate and give comparatively smaller changes in Gibbs free energy ( $\Delta G = \Delta H - T\Delta S$ ) for the process. The effect is seen in numerous systems, but is particularly apparent in aqueous systems where non-covalent interactions dominate. Early work suggested that such correlations might arise as artefacts of inappropriate analysis of experimental data, particularly when using indirect methods, such as van't Hoff analysis of the temperature dependence of equilibrium constants, to determine  $\Delta H$  and  $\Delta S$ , but more direct calorimetric measurements now possible show the same phenomenon. More recently, Dunitz [15] has shown how compensation can be a natural consequence of perturbation of any system comprising a multiplicity of weak non-covalent interactions, of which macromolecular systems in water are just one example. We shall show below how this comes about. In this section we examine this and other quite general sources of entropy–enthalpy compensation.

### 3.1. 'Free energy windows'

Perhaps one of the most surprising aspects of entropy–enthalpy compensation is the way in which it appears even between apparently chemically unrelated species. Our attention was first drawn to this when attempting to rationalise the thermodynamic data obtained from calorimetric measurements on protein–protein interactions in the colicin–porin system [16–18]. These studies involved numerous site-directed mutants and protein fragments, and gave a wide range of binding enthalpies and entropies that proved impossible to rationalise in straightforward structural terms. Despite this, there appeared to be a clear correlation between  $\Delta H$  and  $\Delta S$  of binding obtained for the different species (Fig. 4), suggesting some underlying thermodynamic principle. Even more surprising was the observation that this apparent correlation extended to a much wider range of molecules and different kinds of interaction (Fig.

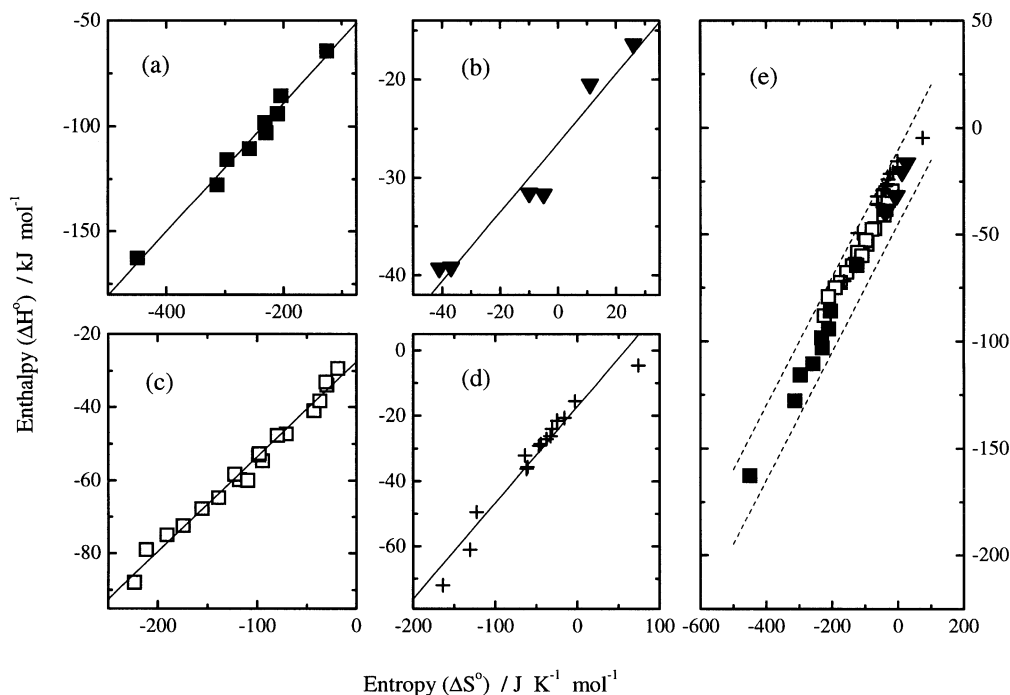


Fig. 4. Examples of entropy–enthalpy compensation in chemically distinct biomolecular species. In all cases the data were obtained by direct calorimetric methods at 25°C. The solid lines indicate linear regression fits with slope close to 300 K. (a) Membrane protein interactions: binding of colicin-TolA mutants and fragments [18,43]; (b) enzyme–substrate complexation: binding of ATP, ADP and 3-phosphoglycerate to phosphoglycerate kinase (PGK) under different buffer conditions [44]; (c) protein–protein interactions: dimerization of insulin in the presence of cyclodextrins [9]; (d) peptide antibiotic interactions: ligand-induced association of vancomycin [7,21]. (e) Combined data from panels a to d. The dashed lines show isoenergetic (constant  $\Delta G^\circ$ ) contours for  $K = 10^2$  to  $10^8$  M<sup>-1</sup> at 300 K.

4), involving peptides and proteins of different sizes and structures, such that almost any pair of  $\Delta H/\Delta S$  values obtained on any system appear likely to fall on a common line, typically with a slope or ‘characteristic temperature’ of approximately 300 K. Similar correlations are found for the thermodynamics of unfolding of a large number of site-directed mutants of different proteins (Fig. 5) [19,20].

Although such correlations between totally unrelated chemical species may appear significant, they are simply a consequence of the limited Gibbs ‘free energy window’ afforded by experimental techniques, and also the limited range of free energies likely to be of functional significance. Although there are no such constraints on possible  $\Delta H$  and  $\Delta S$  values, as shown also re-

cently by Sharp [14], the combination of the two to lie in a finite free energy range gives rise to an apparent linear correlation. This can be shown as follows.

Thermodynamic expressions relating the Gibbs free energy under standard conditions to the equilibrium constant ( $K$ ), standard enthalpy ( $\Delta H^\circ$ ) and entropy ( $\Delta S^\circ$ ),

$$\Delta G^\circ = -RT \ln K = \Delta H^\circ - T\Delta S^\circ$$

rearrange to give:

$$\Delta H^\circ = \Delta G^\circ + T\Delta S^\circ$$

Consequently if, for whatever reason,  $\Delta G^\circ$  were to remain constant, enthalpy/entropy plots would be linear, regardless of the system. Moreover, the

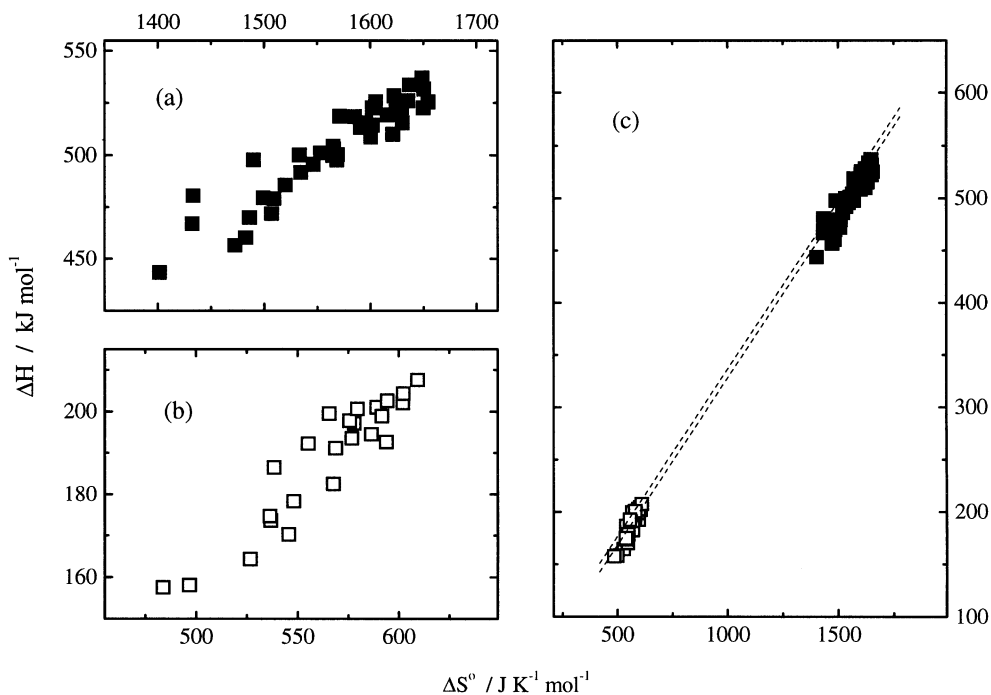


Fig. 5. Examples of enthalpy–entropy compensation in the thermal unfolding stability of globular proteins. Thermodynamic data, determined by two-state analysis of DSC thermograms, are given for a range of barnase [20] and chymotrypsin inhibitor-2 [19] mutants at 320 K. (a) Enthalpy ( $\Delta H$ ) vs. entropy ( $\Delta S$ ) of unfolding of wild type barnase and 41 mutants, measured at pH 3.4–4.4. (b) Wild type Ci2 and 22 mutants, measured at pH 3.0–3.5. (c) Combined data for two different proteins and their mutants. The dashed lines show isoenergetic contours at 320 K for  $\Delta G^\circ = 2-4 \text{ kcal mol}^{-1}$  (8–17  $\text{kJ mol}^{-1}$ ).

slope of such plots would be equal to  $T$ , the absolute temperature of the measurement. Normally, of course,  $\Delta G^\circ$  is not fixed and should be free to vary from system-to-system. However, practical and functional constraints suggest that observed free energies in most systems would usually be confined to a relatively small range of values. For example, instrumental considerations [6] restrict the range of  $K$  values normally accessible from ITC measurements roughly to the range  $K = 10^2$  to  $10^8 \text{ M}^{-1}$ . This corresponds to an observable  $\Delta G^\circ$  range (or ‘window’) of approximately  $-10$  to  $-45 \text{ kJ mol}^{-1}$ . Other experimental methods will have similar limitations. Moreover, for functional and dynamic flexibility in biomolecular interactions,  $K$  values in most systems will be confined to a similar region. Consequently, although not necessarily constant, the range of observable  $\Delta G^\circ$  values is experimentally

limited and may give rise to apparently linear plots. So if, for whatever reason,  $\Delta H$  and/or  $T\Delta S$  are large compared to  $\Delta G$ , then plots of  $\Delta H$  vs.  $\Delta S$  may appear linear, with slope  $\approx T$ . This is illustrated in Figs. 4 and 5, where the dashed lines indicate the limits imposed by the free energy window estimated above. All experimental data collected so far, from a range of calorimetric studies, fall within such windows.

### 3.2. Heat capacity ( $\Delta C_p$ ) and temperature effects

The large temperature dependencies of  $\Delta H$  and  $\Delta S$ , such as seen in Fig. 3, are simply thermodynamic consequences of the significant heat capacity change, or  $\Delta C_p$  effect, associated with such interactions. Regardless of the origin of this  $\Delta C_p$ , simple algebraic considerations show the mere presence of a finite heat capacity can lead to

entropy–enthalpy compensation effects with change in temperature [21]. Recall that the variation of  $\Delta H$  and  $\Delta S$  with respect to some arbitrary reference temperature  $T_{\text{ref}}$  is given by the integral relationships:

$$\Delta H(T) = \Delta H(T_{\text{ref}}) + \int_{T_{\text{ref}}}^T \Delta C_p dT$$

$$\Delta S(T) = \Delta S(T_{\text{ref}}) + \int_{T_{\text{ref}}}^T (\Delta C_p/T) dT$$

If  $\Delta C_p$  is constant, independent of temperature (not necessarily true, but usually a reasonable approximation over a limited temperature range), then integration gives:

$$\Delta H(T) = \Delta H(T_{\text{ref}}) + \Delta C_p(T - T_{\text{ref}})$$

$$\Delta S(T) = \Delta S(T_{\text{ref}}) + \Delta C_p \ln(T/T_{\text{ref}})$$

For small changes in temperature with respect to absolute  $T_{\text{ref}}$ ,  $\delta T = T - T_{\text{ref}}$ , these become:

$$\Delta H(T) = \Delta H(T_{\text{ref}}) + \Delta C_p \delta T$$

$$\begin{aligned} \Delta S(T) &= \Delta S(T_{\text{ref}}) + \Delta C_p \ln(1 + \delta T/T_{\text{ref}}) \\ &\approx \Delta S(T_{\text{ref}}) + \Delta C_p \delta T/T_{\text{ref}} \end{aligned}$$

using the approximation  $\ln(1+x) \approx x$ , for  $x \ll 1$ . Consequently, to the extent that this approximation is valid:

$$\begin{aligned} \Delta G(T) &= \Delta H - T\Delta S \\ &\approx \Delta H(T_{\text{ref}}) - T\Delta S(T_{\text{ref}}) - \Delta C_p \delta T^2/T_{\text{ref}} \\ &= \Delta G(T_{\text{ref}}) \end{aligned}$$

to first order in  $\delta T$ . Moreover, over a limited temperature range for which this approximation is valid:

$$\Delta H(T) \approx \Delta H(T_{\text{ref}}) + T_{\text{ref}}(\Delta S - \Delta S(T_{\text{ref}}))$$

so that a plot of  $\Delta H$  vs.  $\Delta S$  would appear linear with slope  $T_{\text{ref}}$ .

### 3.3. Cooperativity and multiple weak interactions

But this begs the question: why is  $\Delta C_p$  so large in bio/macromolecular systems? Conventionally, large  $\Delta C_p$  effects are associated with hydrophobic interactions [22,23], and the magnitude of  $\Delta C_p$  can be correlated with changes in solvent accessible surface areas ( $\Delta \text{ASA}$ ) in protein folding and other interaction processes [24,25]. But the wider applicability of such  $\Delta C_p/\Delta \text{ASA}$  correlations is now being questioned [10,26–28]. Moreover, Dunitz [15] has shown how such effects are expected for any system made up of a multiplicity of weak interactions, of which hydrophobic interactions are just a special case. More recently, we have shown how similar  $\Delta C_p$  effects may be associated with cooperative hydrogen-bonded networks [29].

This can be seen quite generally as follows. Any (bio)macromolecular transition, such as the unfolding of a globular protein or the dissociation of two subunits, will normally involve the breaking of a cooperative network of interactions that are then replaced by a much less cooperative set of interactions with solvent molecules. The interactions will generally be of a similar type and strength (weak van der Waals, hydrogen bonds, etc.), the major difference being that they act cooperatively in one state and less so in the other. This can be treated theoretically using classical lattice theories of statistical thermodynamics [30], which are also applicable to protein transitions [31].

Picture a lattice of  $N$  molecular units (Fig. 6), where each unit might represent either a water molecule or a peptide group or some other component of the macromolecule, enclosed in a cavity. Assume for simplicity that all these units are identical. Imagine further that each unit may exist in one of two states: either ‘bound’ in some way with its neighbours, or ‘free’ in the sense that interaction with neighbours is broken.

In the absence of any cooperativity, each of these units may be bound or free at random, with

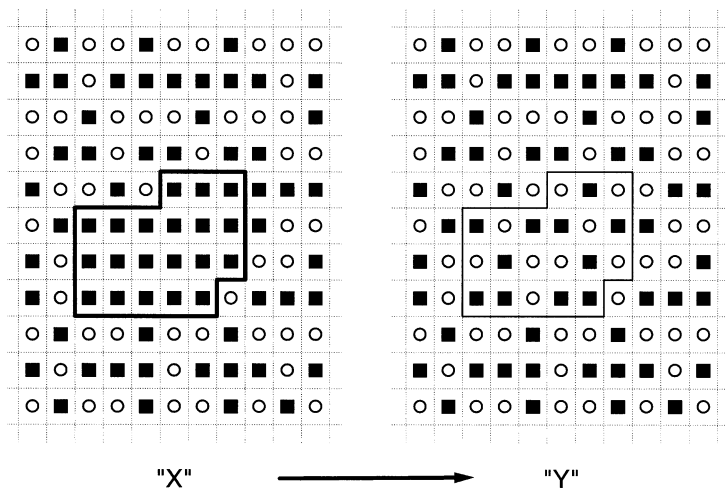


Fig. 6. Sketch illustrating a simple lattice model for cooperative transitions with multiple weak interactions. Each lattice point represents one unit in the system, which may be viewed as either a solvent molecule or a protein group (amino acid residue or smaller component). Each unit may be 'bound' (solid squares) or 'free' (open circles). In state 'X' an number of these (protein) units are cooperatively constrained to the bound state, but in state 'Y' are free to adopt a Boltzmann distribution of bound or free states, just like surrounding solvent.

a statistical probability given by the Boltzmann factor:

$$p(\text{free}) = g \exp(-\varepsilon/RT)$$

where  $\varepsilon$  is the energy difference between 'free' and 'bound' states, and  $g$  is the relative degeneracy of the free unit compared to the bound state (representing the increased configurational freedom of the unit when free of directional interactions with neighbouring groups).  $R$  is the gas constant and  $T$  the absolute temperature. The statistical mechanical partition function for this system ( $Z_Y$ ) will be given by summation over all possible states, bearing in mind the number of permutations of lattice defects:

$$\begin{aligned} Z_Y &= 1 + Np + \{N(N-1)/2\}p^2 + \dots \\ &\quad + \{N!/(N-j)!\}p^j + \dots \\ &= \{1 + g \exp(-\varepsilon/RT)\}^N \end{aligned}$$

using the standard binomial expansion.

Imagine now that, for some reason or other, a small number  $n$  of the total  $N$  are not allowed to be free. This may be because they are all units

within a folded protein, or at the interface between two protein subunits, for example. In this case the partition function is given by:

$$Z_X = \{1 + g \exp(-\varepsilon/RT)\}^{N-n}$$

The transition from state X to state Y represents a cooperative transition in which the  $n$  units, held in the bound state and unable to break free independently of the others, all break simultaneously and join the larger ensemble where they are free to behave non-cooperatively.

Following statistical thermodynamics, the equilibrium constant ( $K$ ) for  $X \rightleftharpoons Y$  is given by the ratio of partition functions:

$$K = Z_Y/Z_X = \{1 + g \exp(-\varepsilon/RT)\}^n$$

from which other thermodynamic functions follow:

Gibbs free energy change:

$$\begin{aligned} \Delta G^\circ &= -RT \ln K \\ &= -nRT \ln \{1 + g \exp(-\varepsilon/RT)\} \end{aligned} \quad (1)$$

Enthalpy change:

$$\Delta H^\circ = RT^2 \partial \ln K / \partial T = ng \varepsilon \exp(-\varepsilon/RT) / \{1 + g \exp(-\varepsilon/RT)\} \quad (2)$$

Heat capacity change:

$$\begin{aligned} \Delta C_p &= \partial \Delta H^\circ / \partial T \\ &= ng \varepsilon^2 \exp(-\varepsilon/RT) \\ & / \left[ RT^2 \{1 + g \exp(-\varepsilon/RT)\}^2 \right] \end{aligned} \quad (3)$$

This simple model illustrates the general thermodynamic principle that positive heat capacity changes are to be expected in any cooperative order–disorder transition involving weakly-interacting units, of which protein unfolding or dissociation of protein subunits are just examples.

Fig. 7 shows typical values using Eqs. (1)–(3) for  $\varepsilon = 3 \text{ kcal mol}^{-1}$  ( $12.5 \text{ kJ mol}^{-1}$ ; cf.  $RT \approx 0.6 \text{ kcal mol}^{-1}$ ;  $1 \text{ cal} = 4.184 \text{ J}$ ),  $g = 50$ , that might be typical order-of-magnitude parameters per amino acid residue (including side-chain motions and interactions) for unfolding of a small (100 residue) globular protein. For comparison, observed  $\Delta C_p$  values for unfolding of globular proteins is approximately  $50 \text{ J K}^{-1} \text{ mol}^{-1}$  per residue, or approximately  $5 \text{ kJ K}^{-1} \text{ mol}^{-1}$  for a protein of this size [29]. Perhaps fortuitously, this simple lattice model also predicts a decrease in  $\Delta C_p$  at higher temperatures similar to that observed for the unfolding of globular proteins. A more detailed treatment of protein unfolding based on a similar hydrogen-bonded network picture emphasises both the qualitative and quantitative agreement that can be found with such models [29].

Order–disorder transitions during protein association/dissociation reactions need not only involve solvation changes. Recent studies [32] have shown how globular proteins behave like ‘surface molten solids’, in which the dense rigid packing of groups in the centre of the protein becomes more fluid and dynamic as one approaches the surface. This is a natural consequence of thermodynamic fluctuations and Brownian motion at the molecular level [33–35]. But it allows one to imagine

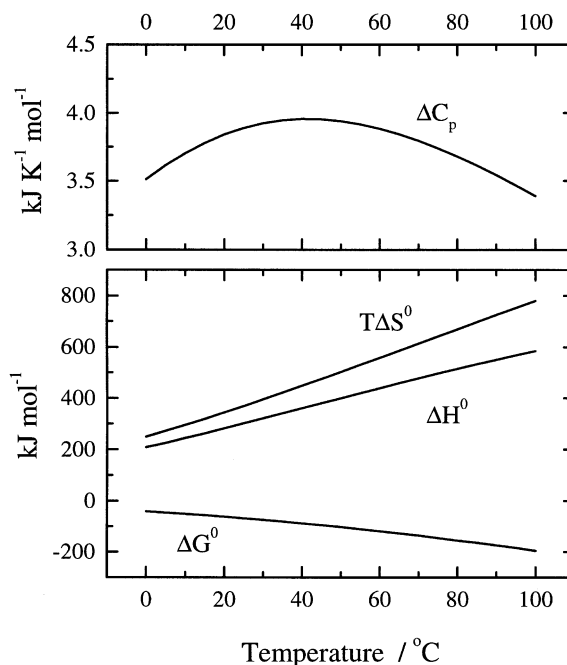


Fig. 7. Lattice model calculations of thermodynamic parameters for a cooperative order–disorder ( $X \rightarrow Y$ ) transition involving 100 weakly interacting units together with a much larger number of similarly interacting solvent units, as might be typical for unfolding of a small globular protein. Calculations based on Eqs. (1)–(3), with  $\varepsilon = 3 \text{ kcal mol}^{-1}$  ( $12.5 \text{ kJ mol}^{-1}$ ) and  $g = 50$ . Parameters are expressed per cooperating unit.

how, during dimerization of two protein subunits for example, surface molten regions of each subunit become buried at the interface, forming a more rigid, less dynamic conformation. Such changes in conformational dynamics will contribute to thermodynamic parameters in just the same way as described above.

### 3.4. Quantum confinement

Quantum mechanical effects are not usually considered to be significant in biomolecular thermodynamics, but there are possible instances where this may not be the case. Any molecular association or assembly process involves the confinement or conformational restriction of atoms or groups, and this can give rise to unexpected effects at the quantum mechanical level. In par-

ticular, once the confinement falls below certain levels, the discrete quantisation of available energy levels for the particle or group in the cavity means that the usual continuum approximation is no longer valid. Moreover, for tightly confined objects, the zero-point energy effects (a consequence of the Heisenberg uncertainty principle) become much more apparent.

This is illustrated in Fig. 8, where we have sketched the energy level diagrams for a point particle confined in one-dimensional boxes of varying dimensions. The ‘particle-in-a-box’ is a classic problem in quantum mechanics, with details available in most physical chemistry texts (e.g. [36]). In such systems the allowed energy levels are given by:

$$E_n = n^2 h^2 / (8mL^2); n = 1, 2, 3 \dots$$

where  $h$  is the Planck constant,  $m$  is the mass of the particle, and  $L$  is the length of the (one-dimensional) box. The actual occupancy of energy levels depends on temperature, according to the Boltzmann probability expression, and the aver-

age thermal energy (per particle) may be evaluated using:

$$\langle E_n \rangle = \sum E_n \exp(-E_n/kT) \quad (4)$$

where  $k$  is the Boltzmann constant and the summation is over all energy levels ( $n = 1, 2, 3 \dots$ ).

As may be seen (Fig. 8), for tightly confined particles the separation between energy levels becomes comparable to or greater than  $kT$ , and the ground-state, zero point energy increases significantly. In the hypothetical case illustrated in Fig. 4 of a particle ‘binding’ to a cavity with potential depth of  $5 \text{ kJ mol}^{-1}$  ( $\approx 2 \text{ kT}$ ), once the cavity size (or particle ‘elbow room’) falls below approximately  $0.2 \text{ \AA}$  the zero point energy effects mean that it is no longer energetically favourable for the particle to fall into this well.

There are temperature dependent effects too. At any temperature above absolute zero there is a finite probability (given by the Boltzmann equilibrium expression) that the particle in the box may be found at energy levels higher than the ground state, but this gets harder the greater the

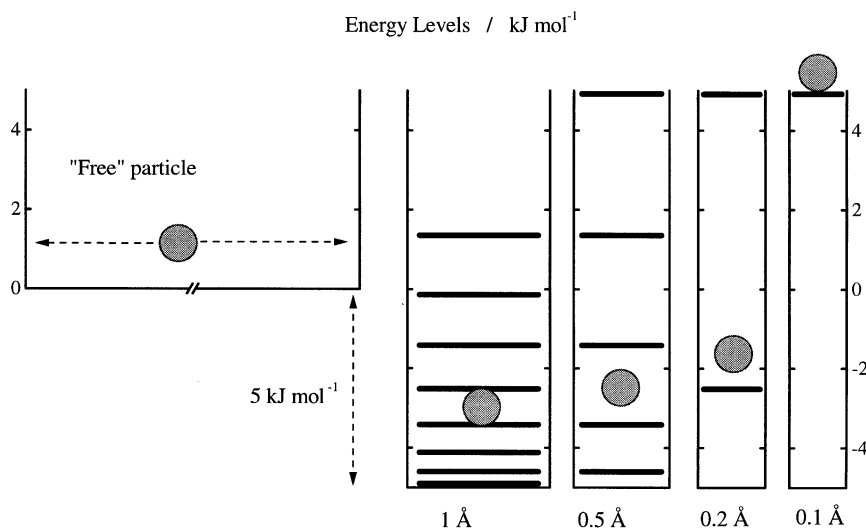


Fig. 8. Effect of quantum confinement on the available energy levels of a particle. This sketch illustrates the hypothetical case of a free particle ( $m = 20 \text{ amu}$ ) falling into different potential energy wells, each of the same depth ( $5 \text{ kJ mol}^{-1}$ ) but with different widths ( $L$ ), corresponding to 1, 0.5, 0.2 and  $0.1 \text{ \AA}$  ‘elbow room’, respectively. The sphere shows the calculated average energy of a particle in each of the boxes with respect to the free particle at room temperature ( $kT = 2.5 \text{ kJ mol}^{-1}$ ). Energy levels are calculated using  $E_n = n^2 h^2 / (8mL^2)$ , and average thermal energies determined by numerical evaluation of the appropriate partition function and Eq. (4).

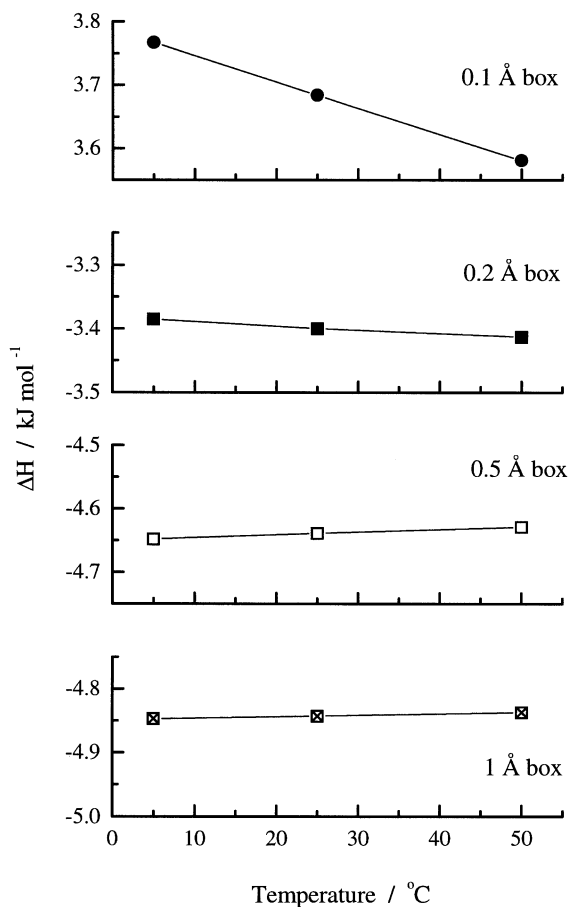


Fig. 9. Quantum confinement effect on the enthalpy of binding of a 20 amu particle in a hypothetical  $5 \text{ kJ mol}^{-1}$  potential well of different dimensions as a function of temperature using Eq. (4).

separation in energy levels compared to  $kT$ . The average energy of a particle in a box at any given temperature can be estimated from the statistical mechanical partition function (see [37], or other standard text for details), as utilised in Eq. (4), and this is also illustrated in Fig. 8. Such average energies will depend on temperature and, consequently, so will the energy of ‘binding’ of the particle to the box from the free particle state. This is plotted for cavities of different size in Fig. 9. This shows that, even for straightforward enclosure of an object in a cavity, with no extraneous solvent or other effects, quantum mechanics imposes restrictions on available energies that trans-

late into a temperature dependence of the energy of interaction: a  $\Delta C_p$  in other words.

Quantum effects of molecular confinement on thermodynamic parameters in weakly interacting systems may be summarised as follows:

- Over and above any other interactions, simple confinement of any particle (molecule) is an endothermic process. This is a quantum effect for which there is no macroscopic interpretation: it is simply a consequence of ‘zero point energy’, arising from the Heisenberg Uncertainty Principle.
- The effects are normally negligible (in macroscopic or covalent systems), but become comparable to  $kT$  (i.e. comparable to non-covalent interactions) when freedom of movement at the molecular level drops below approximately  $0.5 \text{ \AA}$ .
- There is a trade-off between tightness of fit (favourable) and zero point energy (unfavourable).
- $\Delta H_{\text{transfer}}$  (large cavity  $\rightarrow$  smaller cavity) depends on temperature, i.e. it shows a  $\Delta C_p$  effect.
- For ‘loosely-fitting’ cavities,  $\Delta C_p$  is small (and slightly positive). For ‘tightly-fitting’ cavities,  $\Delta C_p$  becomes negative.
- In the limit, for really tight fit ( $\approx 0.1 \text{ \AA}$ ),  $\Delta C_p \rightarrow -3R/2 \approx -12.5 \text{ J K}^{-1} \text{ mol}^{-1}$  (per ‘degree of freedom’).

The magnitude of this effect is comparable to experimental values such as:  $\Delta C_p$  (protein folding) approximately  $-50 \text{ J K}^{-1} \text{ mol}^{-1}$  per residue (each with several degrees of freedom) [29], or the  $\Delta C_p$  associated with protein–protein interaction, burial of non-polar surface area, of approximately  $-1.34 \text{ J K}^{-1} \text{ mol}^{-1} / \text{\AA}^2 \equiv -13 \text{ J K}^{-1} \text{ mol}^{-1}$  per water molecule [24,38]. Consequently it may be important to consider quantum confinement effects when designing close-fitting protein–drug complexes or self-assembling and other related systems.

### 3.5. Hot spots and neutral interactions

The relative insensitivity of many macromolec-

ular systems, at least at the free energy level, to mutations or other chemical changes suggests that many contacts (or interactions) at the macromolecular interface may be thermodynamically neutral. That is, as illustrated by the colicin-porin data, such systems can be surprisingly tolerant to quite large chemical changes. Although mutations may give rise to large changes in  $\Delta H$  and  $\Delta S$ , such changes compensate to give much less of an effect on the  $\Delta G$  of interaction. A corollary of this is that most of the binding affinity (contribution to  $\Delta G$ ) must reside in just one (or a few) crucial locations or ‘hot spots’. One may picture a situation in which just a few contacts at a macromolecular interface might be responsible for the majority of the binding free energy, but that the remainder control stereochemical (structural?) specificity, for example. The latter may make a zero contribution to  $\Delta G$  in the correct conformation (even though  $\Delta H$  and  $\Delta S$  might be finite), but any distortion from the correct configuration would incur a free energy penalty. In such a way, these interactions will be thermodynamically neutral in the sense that they do not contribute to the overall free energy of the interaction, but are nonetheless vital to control the specificity of the complex. Deletion of such ‘neutral’ groups would, thus, not affect the overall  $\Delta G$  of interaction (even though  $\Delta H$  and  $\Delta S$  would change in a complementary fashion), though the specificity might suffer. This is consistent with similar views obtained by structural analysis of protein interfaces [39,40].

### 3.6. Thermodynamic homeostasis

Although, as we have seen, entropy–enthalpy compensation effects seem inevitable in any non-covalent macromolecular interacting system, and indeed frustrate attempts to characterise such interactions, they confer thermodynamic stability and buffering against environmental and mutational challenges that may be of significant advantage in the evolution and function of biomolecular systems. Living organisms depend on a delicate interplay and balance of intermolecular interactions, and anything that upsets this balance

is likely to be a disadvantage in evolutionary terms.

Regardless of the actual molecular origin of entropy–enthalpy compensation, the buffering of thermodynamic free energy that arises in consequence may well be of considerable importance. As illustrated in Fig. 3, in the presence of large  $\Delta C_p$  effects, the temperature variations in  $\Delta H$  and  $\Delta S^\circ$  tend to cancel to give relatively much smaller changes in  $\Delta G^\circ$  and, consequently, smaller changes in  $K$ . In contrast, if  $\Delta H$  and  $\Delta S$  were constant ( $\Delta C_p = 0$ ), then no such compensation would occur and both  $\Delta G^\circ$  and  $K$  would vary much more rapidly with  $T$ . Bearing in mind that biological systems depend on a very delicate balance of interactions, and that the extent of such interaction is determined by  $K$  and  $\Delta G$ , rather than by  $\Delta H$  and  $\Delta S$ , this ‘thermodynamic homeostasis’ would allow a developing or evolving organism to withstand much greater fluctuations in environmental conditions than might otherwise be the case. Similar arguments may be applied to explain stability to (most) random mutations.

Such homeostasis might also be a useful design feature in synthetic self-assembling systems and in attempts at rational drug development. On the one hand, if  $\Delta H/\Delta S$  compensation is unavoidable, then attempts to improve binding affinities ( $\Delta G^\circ$  or  $K$ ) are frustrated by thermodynamic homeostasis. On the other hand, having optimised the binding affinity of one’s ligand or receptor, there may be reasons why one might wish to introduce modifications for other purposes (solubility, stability, antigenicity...) without compromising binding affinity. In such instances thermodynamic homeostasis is a potential advantage.

## 4. Pressure perturbation calorimetry

PPC is a new technique recently introduced by MicroCal LLC [41] that exploits the sensitivity of calorimetric methods to determine volumetric properties in solution. The device is based on DSC, but with the additional facility to apply or release pressure simultaneously to both sample

and reference cells. The inert gas pressure pulses used are relatively small ( $\Delta P$  typically up to  $\pm 5$  atm), and the system measures the difference in heat released ( $\Delta Q$ ) due to pressure–volume changes in the sample and reference solutions under isothermal conditions. For a simple solution (two-component system) the differences arise because the volume occupied by solute molecules in the sample cell is occupied by solvent molecules in the reference cell. This differential heat effect is related to the differences in thermal expansion coefficients ( $\alpha$ ) of solvent and solute in the following way [41]:

$$\Delta Q = -T\Delta P g_s v_s (\alpha_s - \alpha_0)$$

where  $T$  is the absolute temperature,  $g_s$  is the total mass of solute in the sample cell,  $v_s$  (ml/g) is the partial specific volume of the solute, and  $\alpha = (1/v)(\partial v/\partial T)_p$  is the (partial specific) coefficient of thermal expansion of solute ( $\alpha_s$ ) or solvent ( $\alpha_0$ ), respectively.

This has been successfully employed [41] to measure the temperature variation in  $\alpha_s$  for proteins during the thermal unfolding transition, and integration of  $\alpha_s$  vs.  $T$  gives estimates of the change in partial specific volume on unfolding ( $\Delta V_{\text{unf}}$ ) comparable to results from much less convenient high pressure methods. Trial experiments on the unfolding of ubiquitin in mixed methanol/water solvents (Cooper and Jakus, unpublished results) indicate that the volumetric changes associated with thermal unfolding of this small protein disappear at approximately 40% v/v methanol, the same concentration at which the  $\Delta C_p$  effects normally associated with hydrophobic hydration also disappear [42].

However, interpretation of such complex processes is still not easy, and in preliminary experiments we have examined the potentially simpler case of volumetric changes upon ligand (inhibitor) binding to a protein active site. For a multi-component system such as a protein–ligand mixture, measured with respect to a reference cell containing pure solvent (buffer), the magnitude of the PPC heat pulse is given by summation ( $\Sigma$ ) over the individual solute species:

$$\Delta Q = -T\Delta P V_0 \Sigma [S] V_s (\alpha_s - \alpha_0)$$

where  $V_0$  is the volume of the calorimeter cell,  $[S]$  and  $V_s$  are the molar concentrations and partial molar volumes of solutes (S), and quantities have been converted to molar units using:  $g_s v_s = V_0 V_s [S]$ . Summation is over each additional molecular species present in the sample cell. This expression shows how the PPC heat effect depends upon  $V_s(\alpha_s - \alpha_0)$ , the difference in absolute volume thermal expansivity ( $V\alpha = [\partial V/\partial T]_p$ ) between the solute molecule and its equivalent volume occupied by solvent.

For the particular case of enzyme–inhibitor binding (or any other equivalent host–guest complex):



we must compare three different solutions: (a) enzyme alone; (b) inhibitor alone; and (c) enzyme/inhibitor mixture at the same concentrations, in order to determine any changes that take place upon complex formation. If  $C_E$  and  $C_I$  are the total molar concentrations of  $E$  and  $I$ , respectively, and  $V_E$ ,  $V_I$  and  $V_{EI}$  are the associated partial molar volumes of each species, the three heat effects are given by:

Enzyme alone:

$$\Delta Q(a) = -T\Delta P V_0 C_E V_E (\alpha_E - \alpha_0)$$

Inhibitor alone:

$$\Delta Q(b) = -T\Delta P V_0 C_I V_I (\alpha_I - \alpha_0)$$

Enzyme/Inhibitor:

$$\Delta Q(c) = -T\Delta P V_0 \{ [E] V_E (\alpha_E - \alpha_0) + [I] V_I (\alpha_I - \alpha_0) + [EI] V_{EI} (\alpha_{EI} - \alpha_0) \}$$

For comparison, the double-difference may be written as follows:

$$\begin{aligned} \Delta\Delta Q &= \Delta Q(c) - \Delta Q(a) - \Delta Q(b) \\ &= -T\Delta P V_0 [EI] \{ V_{EI} (\alpha_{EI} - \alpha_0) \\ &\quad - V_E (\alpha_E - \alpha_0) - V_I (\alpha_I - \alpha_0) \} \end{aligned}$$

showing that any differential PPC heat effect depends (naturally) on the concentration of enzyme–inhibitor complex formed, and on the difference in volumetric expansivity properties of the complex compared to the free molecules.

Typical data for such an experiment involving binding of a trisaccharide inhibitor (tri-NAG) to hen egg white lysozyme are given in Table 1. These experiments examine the effects on PPC heat pulses of lysozyme in the presence or absence of a tightly binding inhibitor (tri-NAG), determined under the same conditions as used for the ITC binding example shown in Fig. 2, together with some control experiments using a much weaker inhibitor (NAG) and another enzyme (ribonuclease) that does not bind tri-NAG. The first point to note from these preliminary data is that the differential heat effects are very small using these relatively low molecular weight ligands, and must be interpreted with caution whilst we develop a better understanding of PPC and its range of applicability. Nonetheless, it is clear from Table 1 that the binding of tri-NAG to lysozyme does give rise to volumetric changes that are not observed in control experiments with non-binding ligands. In particular, the magnitude of  $\Delta Q$  for the lysozyme/tri-NAG mixture is less exothermic than one would expect from the sum of the individual components, with  $\Delta\Delta Q \approx 3 \mu\text{J}$

under conditions where (using the binding parameters determined in Fig. 2) more than 90% of the protein has inhibitor bound ( $\Delta\Delta Q$  for the non-binding controls are closer to zero, within experimental error).

This suggests that the protein–inhibitor complex expands less with temperature than one would expect for the simple addition of the separate components. There are several possible explanations for this. Firstly one should note that proteins are dynamic, flexible structures, held together in their cooperative (globular) structures by a multiplicity of weak interactions, and subject to quite large thermodynamic fluctuations under the influence of Brownian motion effects of surrounding solvent [33,34]. Indeed, there is a fundamental thermodynamic relationship between thermal expansion coefficient ( $\alpha$ ) and the magnitude of thermal fluctuations in energy and volume in such mesoscopic systems [34]. Binding of ligands to protein active sites is known to reduce conformational fluctuations, usually leading to a more rigid conformation that might have a consequently lower thermal expansivity. But, of course, the situation will be complicated by solvation changes taking place in the protein active site and ligand upon binding. For small molecules in solution, the apparent thermal expansion coefficient is probably dominated by solvation. This is be-

Table 1  
Pressure perturbation calorimetry data for enzyme–inhibitor complexation

Experiment	Contents	$\Delta Q/\mu\text{J}$	$\Delta\Delta Q/\mu\text{J}$	$\alpha/10^{-4} \text{K}^{-1}$
a	Lysozyme	−60.5 (4)		5.70 (3)
b	tri-NAG	−6.3 (5)		2.8 (5)
c	Lysozyme + tri-NAG	−63.7 (5)	3.1 (±1.4)	5.92 (3)
d	NAG	−3.1 (5)		4.7 (4)
e	Lysozyme + NAG	−69.0 (4)	−5.4 (±1.5)	6.21 (3)
f	RNase	−87.1 (5)		7.77 (5)
g	RNase + tri-NAG	−91.7 (5)	1.7 (±1.5)	8.22 (5)

Experimental: Data determined at 20°C in 0.1 M acetate buffer, pH 5.0, using a Microcal PPC system with approximately 60 psi (4 atm) pressure pulses, each experiment comprising multiple pulses (> 20). Proteins (hen egg white lysozyme, ribonuclease A) and inhibitors (*N*-acetyl-glucosamine (NAG), and tri-NAG), obtained from Sigma, were dissolved in buffer and solutions degassed before loading into the PPC cell, with identical buffer as reference. Concentrations used: lysozyme (3.8 mg/ml, 0.26 mM), ribonuclease (4.0 mg/ml), tri-NAG (0.23 mg/ml, 0.35 mM), NAG (0.28 mg/ml) — determined by weight or by 280-nm absorbance, as appropriate. Data are means of multiple determinations, corrected for buffer/buffer controls, with standard errors in final digit(s) given in brackets.

cause the excluded volume of a small molecule by itself, held together solely by covalent bonds and with no secondary or tertiary structure, will respond very little to temperature change, because covalent bond vibrational excitation energies lie well above normal experimental temperatures, and covalent bond lengths will not change much with temperature. The solvation shell around the molecule, however, involves much weaker non-covalent forces and will be much more sensitive to temperature. Consequently, at least for small rigid ligands, volumetric changes upon binding are likely to reflect mainly changes in solvation. Removal of the hydration layer around tri-NAG upon binding to lysozyme is therefore likely to reduce the overall thermal expansivity, as observed.

## 5. Conclusions

Calorimetric techniques yield detailed information about the thermodynamics of biomolecular interactions, in which solvation plays a major role, but interpretation in terms of specific interactions is frustrated by the lack of characteristic thermodynamic signatures and by ubiquitous entropy–enthalpy compensation.

There are numerous reasons for entropy–enthalpy compensation, but the thermodynamic homeostasis that results may be of evolutionary significance in allowing adaptation to harsher environments.

Limited free energy windows, conditioned either by experimental limitations or by functional relevance, give rise to apparent entropy–enthalpy compensation even between chemically unrelated species.

Heat capacity effects, which give rise to entropy–enthalpy compensation in the temperature domain, are an inevitable consequence in cooperative systems comprising networks of weakly interacting units.

Even in the absence of specific interactions, molecular confinement can give rise to quantum zero-point energy effects and temperature dependence of enthalpies.

Pressure perturbation calorimetry of protein–

ligand complexes shows how changes in thermal expansion properties may be related to changes in macromolecular conformational dynamics and solvation.

## Acknowledgements

This work was supported in part by funding from BBSRC, EPSRC and the Medical Research Council. We are grateful to the Wellcome Trust for research studentship support under the 4-year PhD scheme (Nöllmann), and to Margaret Nutley for technical assistance.

## References

- [1] J.M. Sturtevant, The thermodynamic effects of protein mutations, *Curr. Opin. Struct. Biol.* 4 (1994) 69–78.
- [2] A. Cooper, Thermodynamic analysis of biomolecular interactions, *Curr. Opin. Chem. Biol.* 3 (1999) 557–563.
- [3] V.V. Plotnikov, J.M. Brandts, L.N. Lin, J.F. Brandts, A new ultrasensitive scanning calorimeter, *Anal. Biochem.* 250 (1997) 237–244.
- [4] A. Cooper, M.A. Nutley, A. Wadood, Differential scanning microcalorimetry in: S.E. Harding, B.Z. Chowdhry (Eds.), *Protein–Ligand Interactions: Hydrodynamics and Calorimetry*, Oxford University Press, Oxford, New York, 2000, pp. 287–318.
- [5] G.I. Makhatadze, P.L. Privalov, Energetics of protein structure, *Adv. Protein Chem.* 47 (1995) 307–425.
- [6] T. Wiseman, S. Williston, J.F. Brandts, L.N. Lin, Rapid measurement of binding constants and heats of binding using a new titration calorimeter, *Anal. Biochem.* 179 (1989) 131–137.
- [7] A. Cooper, K.E. McAuley-Hecht, Microcalorimetry and the molecular recognition of peptides and proteins, *Philos. Trans. R. Soc. Lond. Ser. A-Math. Phys. Eng. Sci.* 345 (1993) 23–35.
- [8] A. Cooper, Microcalorimetry of protein–DNA interactions in: A. Travers, M. Buckle (Eds.), *DNA–Protein Interactions*, Oxford University Press, Oxford, 2000, pp. 125–139.
- [9] A. Lovatt, A. Cooper, P. Camilleri, Energetics of cyclodextrin-induced dissociation of insulin, *Eur. Biophys. J.* 24 (1996) 354–357.
- [10] C. Frisch, G. Schreiber, C.M. Johnson, A.R. Fersht, Thermodynamics of the interaction of barnase and barstar: Changes in free energy versus changes in enthalpy on mutation, *J. Mol. Biol.* 267 (1997) 696–706.
- [11] A. Cooper, Microcalorimetry of protein–protein interactions in: J.E. Ladbury, B.Z. Chowdhry (Eds.), *Biocalorimetry: The Applications of Calorimetry in the Biological Sciences*, Wiley, 1998, pp. 103–111.
- [12] S. Knapp, M. Zamai, D. Volpi et al., Thermodynamics of

- the high-affinity interaction of TCF4 with  $\beta$ -catenin, *J. Mol. Biol.* 306 (2001) 1179–1189.
- [13] R. Lumry, S. Rajender, Enthalpy–entropy compensation phenomena in water solutions of proteins and small molecules: a ubiquitous property of water, *Biopolymers* 9 (1970) 1125–1227.
- [14] K. Sharp, Entropy–enthalpy compensation: Fact or artefact? *Protein Sci.* 10 (2001) 661–667.
- [15] J.D. Dunitz, Win some, lose some — enthalpy–entropy compensation in weak intermolecular interactions, *Chem. Biol.* 2 (1995) 709–712.
- [16] L.J.A. Evans, S. Labeit, A. Cooper, L.H. Bond, J.H. Lakey, The central domain of colicin N possesses the receptor recognition site but not the binding affinity of the whole toxin, *Biochemistry* 35 (1996) 15143–15148.
- [17] L.J.A. Evans, A. Cooper, J.H. Lakey, Direct measurement of the association of a protein with a family of membrane receptors, *J. Mol. Biol.* 255 (1996) 559–563.
- [18] E.M. Raggett, G. Bainbridge, L.J.A. Evans, A. Cooper, J.H. Lakey, Discovery of critical tol A-binding residues in the bactericidal toxin colicin N: a biophysical approach, *Mol. Microbiol.* 28 (1998) 1335–1343.
- [19] S.E. Jackson, M. Moracci, N. Elmasry, C.M. Johnson, A.R. Fersht, Effect of cavity-creating mutations in the hydrophobic core of chymotrypsin inhibitor-2, *Biochemistry* 32 (1993) 11259–11269.
- [20] C.M. Johnson, M. Oliveberg, J. Clarke, A.R. Fersht, Thermodynamics of denaturation of mutants of barnase with disulfide crosslinks, *J. Mol. Biol.* 268 (1997) 198–208.
- [21] D. McPhail, A. Cooper, Thermodynamics and kinetics of dissociation of ligand-induced dimers of vancomycin antibiotics, *J. Chem. Soc.-Faraday Trans.* 93 (1997) 2283–2289.
- [22] W. Kauzmann, Some factors in the interpretation of protein denaturation, *Adv. Protein Chem.* 14 (1959) 1–63.
- [23] K.A. Dill, Dominant forces in protein folding, *Biochemistry* 29 (1990) 7133–7155.
- [24] J.R. Livingstone, R.S. Spolar, M.T. Record, Contribution to the thermodynamics of protein folding from the reduction in water-accessible nonpolar surface-area, *Biochemistry* 30 (1991) 4237–4244.
- [25] R.S. Spolar, J.R. Livingstone, M.T. Record, Use of liquid-hydrocarbon and amide transfer data to estimate contributions to thermodynamic functions of protein folding from the removal of nonpolar and polar surface from water, *Biochemistry* 31 (1992) 3947–3955.
- [26] E.R. Guinto, E. Di Cera, Large heat capacity change in a protein-monovalent cation interaction, *Biochemistry* 35 (1996) 8800–8804.
- [27] B. Kuhlman, D.P. Raleigh, Global analysis of the thermal and chemical denaturation of the N-terminal domain of the ribosomal protein L9 in H<sub>2</sub>O and D<sub>2</sub>O. Determination of the thermodynamic parameters,  $\Delta H^\circ$ ,  $\Delta S^\circ$ , and  $\Delta C_p$ , and evaluation of solvent isotope effects, *Protein Sci.* 7 (1998) 2405–2412.
- [28] D.A. Henriques, J.E. Ladbury, R.M. Jackson, Comparison of binding energies of SrcSH2-phosphotyrosyl peptides with structure-based prediction using surface area based empirical parameterization, *Protein Sci.* 9 (2000) 1975–1985.
- [29] A. Cooper, Heat capacity of hydrogen-bonded networks: an alternative view of protein folding thermodynamics, *Biophys. Chem.* 85 (2000) 25–39.
- [30] J.O. Hirschfelder, C.F. Curtiss, R.B. Bird, *Molecular Theory of Gases and Liquids*, Wiley, New York, 1954.
- [31] K.A. Dill, S. Bromberg, K.Z. Yue et al., Principles of protein-folding — a perspective from simple exact models, *Protein Sci.* 4 (1995) 561–602.
- [32] Y. Zhou, D. Vitkup, M. Karplus, Native proteins are surface molten solids: application of the Lindemann criterion for solid versus liquid state, *J. Mol. Biol.* 285 (1999) 1371–1375.
- [33] A. Cooper, Thermodynamic fluctuations in protein molecules, *Proc. Natl. Acad. Sci. USA* 73 (1976) 2740–2741.
- [34] A. Cooper, Protein fluctuations and the thermodynamic uncertainty principle, *Prog. Biophys. Mol. Biol.* 44 (1984) 181–214.
- [35] A. Cooper, Conformational change, fluctuation and drift in biological macromolecules — an empirical Langevin approach, *J. Mol. Liq.* 39 (1988) 195–206.
- [36] P.W. Atkins, *Physical Chemistry*, 5th ed., Oxford University Press, Oxford, 1994.
- [37] D.A. McQuarrie, *Statistical Mechanics*, Harper & Row, New York, London, 1976.
- [38] R.S. Spolar, J.H. Ha, M.T. Record, Hydrophobic effect in protein folding and other noncovalent processes involving proteins, *Proc. Natl. Acad. Sci. USA* 86 (1989) 8382–8385.
- [39] A.A. Bogan, K.S. Thorn, Anatomy of hot spots in protein interfaces, *J. Mol. Biol.* 280 (1998) 1–9.
- [40] C.K. Vaughan, A.M. Buckle, A.R. Fersht, Structural response to mutation at a protein–protein interface, *J. Mol. Biol.* 286 (1999) 1487–1506.
- [41] MicroCal, Pressure Perturbation Calorimetry application note, <http://www.microcalorimetry.com/> (2000), (MicroCal, LLC, 22 Industrial Drive East, Northampton, MA 01060-02327 USA).
- [42] D.N. Woolfson, A. Cooper, M.M. Harding, D.H. Williams, P.A. Evans, Protein folding in the absence of the solvent ordering contribution to the hydrophobic interaction, *J. Mol. Biol.* 229 (1993) 502–511.
- [43] I. Gokce, E.M. Raggett, Q. Hong, R. Virden, A. Cooper, J.H. Lakey, The TolA-recognition site of colicin N. ITC, SPR and stopped-flow fluorescence define a crucial 27-residue segment, *J. Mol. Biol.* 304 (2000) 621–632.
- [44] K.E. McAuley-Hecht, A. Cooper, Microcalorimetry of enzyme-substrate binding-yeast phosphoglycerate kinase, *J. Chem. Soc.-Faraday Trans.* 89 (1993) 2693–2699.